Genetic and molecular characterization reveals a unique nucleobase cation symporter 1 in Arabidopsis

George S. Mourad [a],*, Julie Tippmann-Crosby [a], Kevin A. Hunt [a], Yvonne Gicheru [a], Kaely Bade [a], Tyler A. Mansfield [a], Neil P. Schultes [b]

[a] *Department of Biology, Indiana University–Purdue University Fort Wayne, 2101 East Coliseum Blvd., Fort Wayne, IN 46805, USA*
[b] *Department of Biochemistry & Genetics, The Connecticut Agricultural Experiment Station, 123 Huntington St., New Haven, CT 05611, USA*

ARTICLE INFO

ABSTRACT

Locus At5g03555 encodes a nucleobase cation symporter 1 (AtNCS1) in the Arabidopsis genome. Arabidopsis insertion mutants, *AtNcs1-1* and *AtNcs1-3*, were used for in planta toxic nucleobase analog growth studies and radio-labeled nucleobase uptake assays to characterize solute transport specificities. These results correlate with similar growth and uptake studies of *AtNCS1* expressed in *Saccharomyces cerevisiae.* Both in planta and heterologous expression studies in yeast revealed a unique solute transport profile for AtNCS1 in moving adenine, guanine and uracil. This is in stark contrast to the canonical transport profiles determined for the well-characterized *S. cerevisiae* NCS1 proteins FUR4 (uracil transport) or FCY2 (adenine, guanine, and cytosine transport).
© 2012 Federation of European Biochemical Societies. Published by Elsevier B.V. All rights reserved.

1. Introduction

In plants, nucleobases play a pivotal role in metabolism, growth, and development. Nucleic acid metabolism, carbohydrate, glycoprotein and phospholipid metabolism as well as the biosynthesis of many secondary metabolites, such as cytokinins, theobromine and caffeine, are just a few examples of the myriad of biochemistries dependent upon nucleobases [1–4]. Nucleobase biochemistry is marked by a sophisticated interaction between salvage reactions, de novo synthesis and catabolism pathways. A further trait in nucleobase biochemistry is the high degree of compartmentalization, necessitating extensive intra- and inter-cellular transport. A prime example is the essential interplay of nucleobase biochemical pathways in seed germination and early seedling development necessitating both intercellular transport of metabolites from endosperm to cotyledons as well as intracellular transport between organelles [1–7]. This highly involved nucleobase transport serves the numerous needs for nucleobases in plants and stands in contrast to nucleobase transport in microbes that mainly serves salvaging of external nitrogen sources.

The extent and importance of nucleobase transport is reflected in the Arabidopsis genome which contains six different gene families encoding for nucleobase transporters. Two transporter families are unique to plants and include the purine permease (PUP) with 21 members and ureide permease (UPS) with eight members. Characterized Arabidopsis PUP proteins transport adenine, cytosine or secondary compounds such as cytokinins and caffeine [8–10]. Two transporters in the Arabidopsis UPS family transport uracil, allantoin and the purines xanthine and hypoxanthine [11–13], and an UPS from French bean transports allantoin [14]. The remaining four nucleobase transporter families have orthologs in other prokaryotic and eukaryotic taxa. Nucleobase-ascorbate transporters (NATs) are ubiquitous and collectively transport an array of solutes including purines, oxidized purines (xanthine, hypoxanthine, and uric acid), uracil and ascorbate [15,16]. Although none of the 12 identified Arabidopsis NAT loci are functionally-characterized yet, the maize Leaf Permease 1 is known to transport xanthine and uric acid [17,18]. The AzgA-like transporter family in Arabidopsis facilitates the movement of adenine, guanine and uracil [19]. What appears to be the only member of the nucleobase cation symporter 1 (NCS) is encoded by Arabidopsis locus At5g03555 which encodes a protein with significant amino acid similarity to FUR4, a uracil transporter of *Saccharomyces cereviciae* [20].
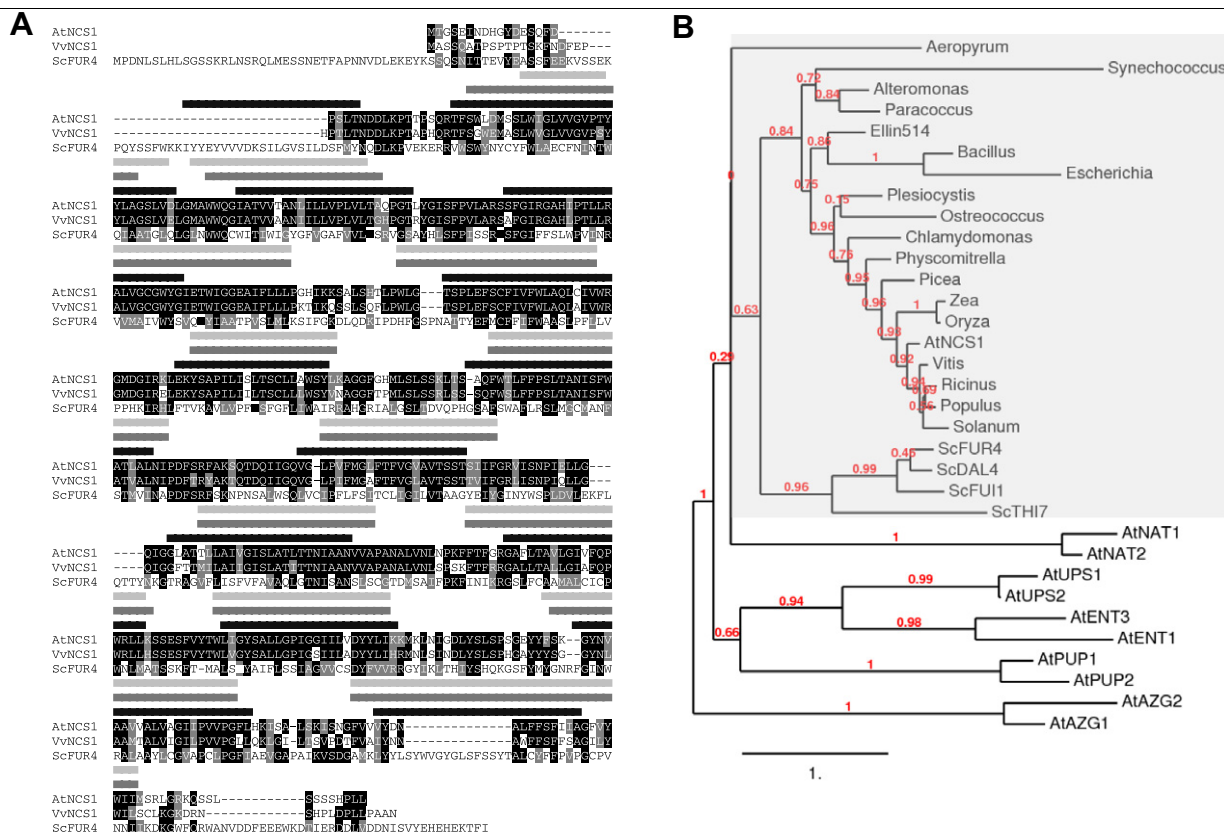

Fig. 1. Amino acid sequence similarity and phylogenetic relationships of AtPRT1. (A) Alignment of AtNCS1 (GenBank # AAL25608.1), a paralog from *Vitus vinifera* (XP_002264940.1) [VvNCS1] and the uracil transporter from *Saccharomyces cerevisiae* ScFUR4 (NP_009577) by ClustalW [45]. Black boxes represent amino acid identity while grey boxes indicate amino acid similarity. Predicted transmembrane spanning domains are indicated for AtNCS1 (light gray bars), VtNCS1 (dark gray bars) and ScFUR4 (black bars) using TMHMM [29]. (B) Phylogenetic relationships of select NCS1 proteins (in grey shaded area) from eukaryotes [*Chlamydomonas reinhardtii* (XP_001694932.1); *Physcomitrella patens* (XP_001758782.1); *Picea glauca* (UGID:3879008); *Plesiocystis pacifica SIR-1* (ZP_01906283.1); *Populus trichocarpa* (XP_002326396.1); *Oryza sativa* (NP_001047676.1); *Ostreococcus lucimarinus* (XP_001418566.1); *Ricinus communis* (XP_002519429.1); *Solanum lycopersicum* (translated from AK323376)]; *Zea mays* (NP_001136535.1); and *Saccharomyces cerevisiae* ScDal4 (NP_012294), ScFUR4 (NP_009577), ScThi7 (NP_013338), ScFUI1 (NP_009511)], and prokaryotes [*Alteromonas macleodii* (ZP_01111046); *Bacillus subtilis* (NP_391528.1); bacterium Ellin514 (ZP_03630186.1), *Escherichia coli* (AP_001159.1), *Paracoccus denitrificans* (ZP_00631515), Synechococcus sp. PCC 7335 (ZP_05037138.1), *Aeropyrum pernix* (NP_147909.1)] with representative members of other Arabidopsis nucleobase transporters; AtAZG1 (AAQ65179.1), AtAZG2 (BAB09401.1), AtENT1 (NP_564987), AtENT3 (NP_192421), AtNAT1 (Q9SHZ3.1), AtNAT2 (Q94C70.2), AtPUP1 (NP_174144.1), AtPUP2 (NP_973592.1), AtUPS1 (NP_565303.1), AtUPS2 (NP_178451.2). Red numbers at nodes denote branch support values and the scale bar denotes genetic distance of branch length. Phylogenetic tree constructed using Phylogeny.fr [46] using MUSCLE alignment parameter [47] and Tree construction using maximum likelihood [48–50].

Although each plant nucleobase transporter has a unique solute transport specificity and gene expression pattern, the emerging picture from available data reveals a dense system of overlapping transport throughout the plant. Here we add to this picture by characterizing the sole *Arabidopsis thaliana* NCS gene (AtNCS1) through in planta radiolabel studies using insertion mutants as well as through heterologous complementation studies in yeast.

2. Materials and methods

2.1. Arabidopsis genetic stocks and growth conditions

Arabidopsis lines WiscDsLox419Co3 [ABRC # CS854962] [21], and GK-266G10 [ABRC# CS305244] [22], were obtained from Arabidopsis Biological Resource Center (Columbus, OH, USA) and line ET8162 from Cold Spring Harbor Laboratory (Cold Spring Harbor, NY, USA) [23]. Growth conditions were as previously described [19]. For the allantoin growth experiments, MAM was used in which 5 mM allantoin was the sole nitrogen source as previously described [11].

2.2. Molecular manipulations

Arabidopsis DNA was extracted using DNeasy Plant Mini Kit (Qiagen, Valencia, CA, USA) or QuickExtract (Epicentre, Madison, WI, USA). Individual plants from insertion lines GK-266G10, ET8162 and WiscDsLoc419Co3 were genotyped by multiplex PCR using gene-specific primers (F12E4C, F12E4G, LP-03555 or RP-03555) and T-DNA specific primers (GABITDNA, Ds3-2 or P745) (Table 1). Total RNA was isolated using TRIzol Reagent (Invitrogen, Carlsbad, CA, USA) from tissues at different developmental stages. Reverse transcription was performed using Reverse Transcriptase M-MuLV (Roche, Basel, Switzerland) at 42 °C for 2 h and then

Table 1
Oligonucleotide primers used in this study.

| Oligonucleotide	DNA sequence (5′–3′)
At5g03555YEA	CCGCTCGAGATGACCGGCTCAGAAATTAATG
At5g03555YEB	ACATGCATGCTTACAAAAGCGGATGTGAAGA
AtACT2A	TCCTCACTTTCATCAGCCG
AtACT2B	ATTGGTTGAATATCATCAGCC
Ds3-2	CGATTACCGTATTTATCCCGTTC
F12E4C	AAGCTTCATCTTCAGAAGCCAAAAGGTTGG
F12E4D	GCCGCTCGAGATGACCGGCTCAGAAATTAATGAC
F12E4E	TACATGCATGCTTACAAAAGCGGATGTGAAGAAGA
F12E4G	GGATCCCGCTGAGAGTCGTGGGCGGATGAC
GABITDNA	ATATTGACCATCATACTCATTGC
LP-03555	GAATTTCCTTCCCTGTCCTTG
RP-03555	CCGGAGGGACTCAAAGAGTAC
P745	AACGTCCGCAATGTGTTATTAAGTTGTC
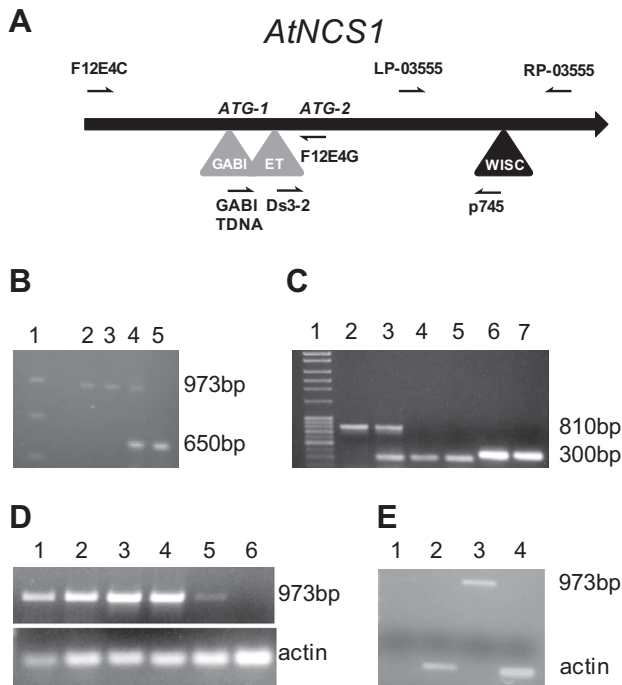
Fig. 2. Molecular analysis of the At5g03555 locus. (A) Physical map of locus At5g03555 (*AtNCS1*) is delineated by the solid arrow. *ATG* indicates predicted start codon. The name, position and 5′–3′ direction of oligonucleotide primers are given. Triangles indicate positions of WiscDsLox419Co3 (WISC), GK-266G10 (GABI) and ET8162 (ET) T-DNA insertions. PCR fragment sizes of informative oligonucleotide combinations are given for genotyping and transcript detection. (B) Genotype analysis of the WISC line segregating for the *AtNcs1-1* insertion. Lane 1 contains molecular size standards, lanes 2 and 3 show *AtNCS*1-specific DNA fragments (973 bp) representative of homozygous wild type individuals, lane 4 heterozygous *AtNCS1/AtNcs1-1* (973 bp and 650 bp) individual and lane 5 individual homozygous for the insertion *AtNcs1-1*. (C) Lanes 2–5 show genotypes of *AtNcs1-3* segregating family, an *AtNCS1/AtNCS1* wild type (lane2), a heterozygous *AtNCS1/AtNcs1-3* individual (lane 3), *AtNcs1-3/AtNcs1-3* individuals (lanes 4 and 5), while lanes 6 and 7 show the genotypes of two homozygous *AtNcs1-2* individual plants. (D) RT-PCR analysis of *AtNCS1* (973 bp) and actin RNA isolated from Columbia wild type 5-day-old seedlings (lane 1), 10-day-old seedlings (lane 2), isolated flowers (lane 3), inflorescence (lane 4), mature leaf (lane 5), and *AtNcs1-1/ AtNcs1-1* 10-day-old seedlings (lane 6). (E) RT-PCR analysis of *AtNCS1* (lanes 1 and 3) and actin (lanes 2 and 4) RNA isolated from *AtNcs1-3/AtNcs1-3* (lanes 1 and 2) and from Columbia wild type (lanes 3 and 4) 10-day-old seedlings.

treated with DNA-free (Ambion, Austin, TX, USA). Subsequent PCR amplification with Taq DNA Polymerase (Qiagen) using oligonucleotides LP-03555 and RP-03555 or *AtACT2A* and *AtACT2B* was performed for 30 cycles of 94 °C 30 s, 55 °C 30 s and 70 °C 2 min in a Mastercycler gradient machine (Eppendorf, Hamburg, Germany). Genomic DNA from Arabidopsis Columbia wild type was amplified with primers At5g03555YEA and At5g03555YEB and the resulting DNA fragment treated with *Xho* I and *Sph* I, ligated with *Xho* I/*Sph* I linearized pRG399 [19] to form plasmid pRH369. Plasmid pRH124 is composed of the pRG399 yeast expression vector containing a 1.8 kb insert consisting of an open reading frame that encodes for the 599 amino acid version of AtNCS1. This plasmid was constructed by PCR-amplifying bacterial artificial chromosome F12E4 containing genomic sequence of At5g03555 with oligonucleotides F12E4D and F12E4E. The resulting DNA fragment was digesting with *Xho* I and *Sph* I and ligated into the like cleaved sites on pRG399. The plasmid insert was subject to DNA sequence to verify sequence integrity.

2.3. Yeast cultures and transformation

Saccharomyces cerevisiae strains FY1679-5C [*MAT α leu2Δ1 his3Δ200 ura3-52*] [24] and RG191 [Mat α, *fcy2Δ:: kanMX4, his3Δ1,*
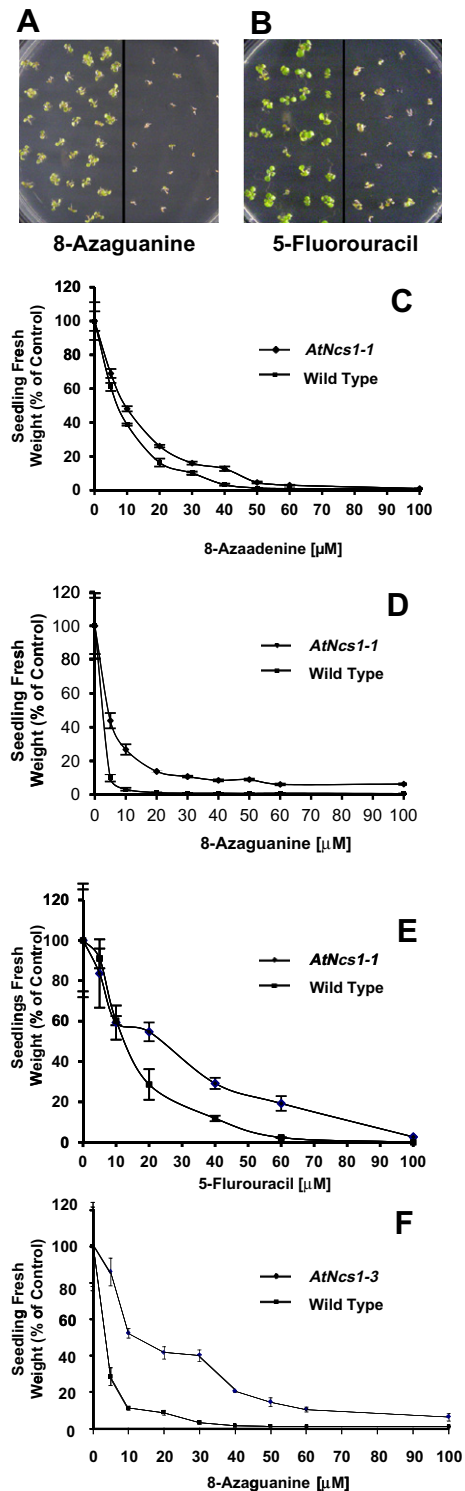

Fig. 3. Growth of *AtNcs1-1* mutant and Columbia wild type on toxic purine or pyrimidine analogs. Ten-day-old *AtNcs1-1/AtNcs1-1* (left side) and Columbia wild type (right side) seedlings grown in MAM agar medium supplemented with 5 μM 8-azaguanine (A) or 80 μM 5-fluorouracil (B). Effect of a concentration series of toxic purine and pyrimidine analogs on the fresh weight of *AtNcs1-1* (C–E), *AtNcs1-3* (F) mutants, and Columbia wild type 10-day-old seedlings grown in MAM agar growth medium supplemented with 8-azaadenie (C), 8-azaguanine (D and F), or 5-fluorouracil (E).

leu2Δ0, met15Δ0, ura3Δ0] [25] and NC122-sp6 [*Mat α leu2 fur4Δ*] [20] were grown in YPD or on Synthetic Complete medium (SC) at 30 °C. Yeast transformation was by the lithium acetate method

Table 2
Resistance of *AtNcs1-1* mutants to a panel of toxic purine and pyrimidine analogues incorporated in the agar growth medium (+ = resistance; − = sensitive).

Toxic analog	*AtNcs1-1*
8-Azaadenine	+
8-Azaguanine	+
5-Bromo-2′-deoxyuridine	−
5-Fluorocytosine	−
5-Fluoro-2′-deoxyuridine	−
5-Fluoroorotic acid	−
5-Fluorouracil	+
Pyrithiamine	−
Allantoin	−

[26]. Sensitivity to toxic nucleobase analogues was assayed by adding filter-sterilized stock solutions to the growth media.

2.4. Radiolabel uptake experiments

Five- and eleven-day-old seedlings were transferred from MAM onto MAM supplemented with [8-^{3}H]guanine (3.7 kBq ml^{-1}), [2,8-^{3}H]adenine (3.7 kBq ml^{-1}) or [5,6-^{3}H]uracil (12.33 kBq ml^{-1}) (Moravek Biochemicals, Brea, CA) or MAM alone as previously described [19]. After 2 days of growth the plants were carefully removed and weighed. Three 75 mg samples of selected genotype tissue were homogenized in 0.5 ml 20 mM Tris–HCl, pH 8. After homogenization, samples were centrifuged at 11,750g for a minute. For each sample, the radioactivity in 0.1 ml of extract was determined by mixing with 3 ml EcoLume (MP Biochemicals, Solon, OH) and measured by using a scintillation counter. For radiolabeled uptake experiments in yeast, cells were grown to OD$_{600}$ = 4 and incubated for 0 and 2.5 min with 0.5 μM of one of the isotopes mentioned above in 100 mM citrate buffer (pH 3.5) with 1% glucose. Fifty microliter aliquots were added to 4 mL of ice-cold water and filtered through a 0.45 μm Metricel membrane filter (Gelman Sciences, Ann Arbor, MI). Filters were then washed with 8 ml of water and radioactivity was measured by scintillation counter.

2.5. Transport kinetics of AtNCS1 expressed in yeast

Time course for the uptake of 0.5 μM [5,6-^{3}H]uracil was performed with yeast cells (OD$_{600}$ = 4) expressing AtNCS1-1. Substrate saturation kinetics was established for varying concentrations of [5,6-^{3}H]uracil and [2,8-^{3}H]adenine at 2.5 min using yeast cells (OD$_{600}$ = 4) expressing AtNCS1-1. Radiolabel uptake was assayed as mentioned above.

2.6. Radionucleobase uptake by yeast expressing AtNCS1-1 with a protonophore

Yeast suspensions were prepared as described [19]. Equal volumes (50 μL) of yeast suspension (OD$_{600}$ = 2) and buffer containing 1.0 μM [5,6-3H]uracil (12.33 kBq ml^{-1}) and 100 μM carbonyl cyanide m-chlorophenylhydrazone (CCCP) in 100 mM citrate buffer (pH 3.5) with 1% glucose. For control, CCCP was omitted from the reaction mixture. Assay of radiolabel uptake was performed at 0 and 2.5 min as mentioned above.

3. Results and discussion

3.1. Arabidopsis locus At5g03555 encodes for AtNCS1

The Arabidopsis genome contains a locus (At5g03555) that encodes for a protein with sequence and structural characteristics common with members of the purine related transporters or nucleobase cation symporter 1 (NCS1) superfamily. At5g03555 is
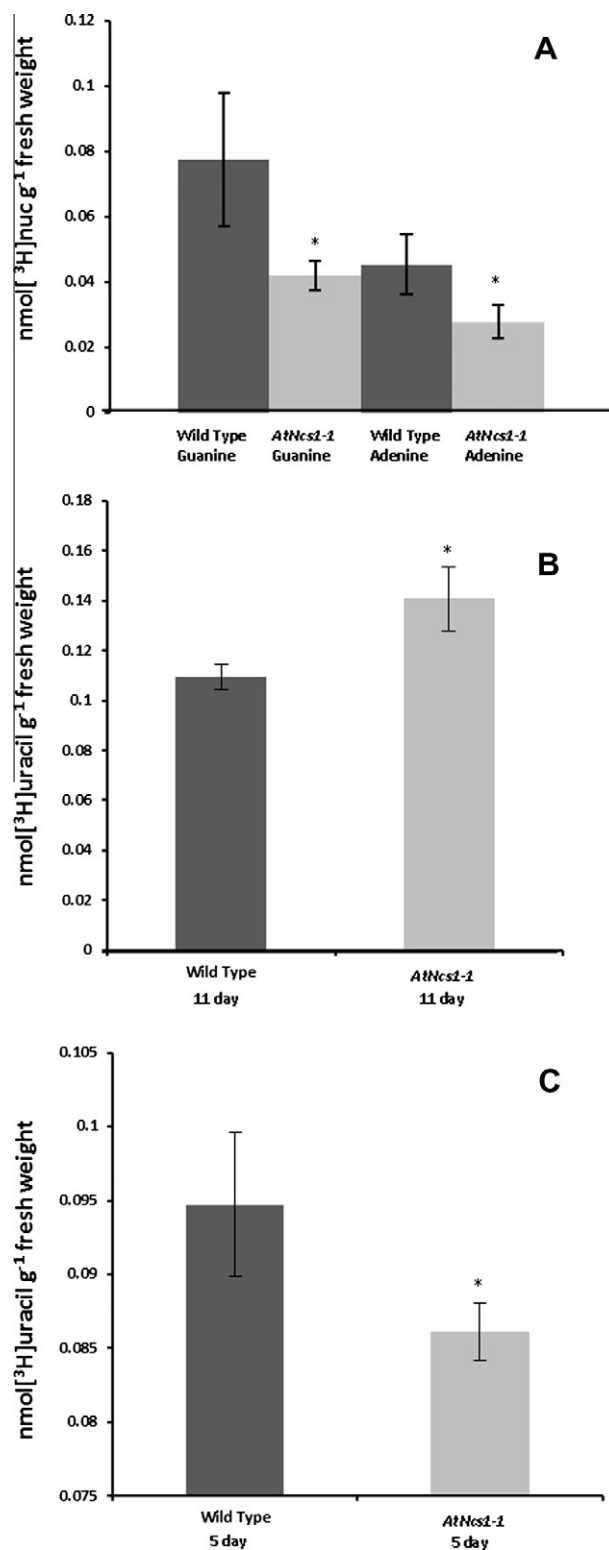

Fig. 4. Uptake of [^{3}H]-adenine, -guanine, and -uracil by *AtNcs1-1* mutant and Columbia wild type seedlings. Radio-labeled purine uptake was measured in extracts from 11-day-old seedlings (A). Radio-labeled uptake of uracil was measured in extracts of 11-day-old (B) and 5-day-old (C) seedlings. Values shown are the mean of three independent experiments. Error bars indicate the standard error of the mean. Statistical analysis used an independent paired *t*-test. Significance was measured at *P = 0.05.

therefore renamed as the *A. thaliana* nucleobase cation symporter 1 or AtNCS1. Despite the extensive evolutionary distance between plants and yeast, AtNCS1 shares substantial amino acid similarity

(20–22% amino acid identity and 52–54% amino acid similarity) to the well characterized *S. cerevisiae* NCS1 FUR4 family including FUR4 (uracil transporter), DAL4 (allantoin transporter), FUI1, (uridine transporter), THI7, (thiamine transporter) and lesser levels of sequence similarity to the related NCS1 FCY2 family including the cytosine–adenine transporters FCY2, 21 and 22 and vitamin B6 transporter, TPN1 (Fig. 1A) [15,16,27,28]. Secondary structure predictions suggest that AtNCS1 and a closely related orthologous protein from *Vitus vinifera*, are membrane localized proteins showing twelve predicted membrane spanning domains (Fig. 1A) [29]. Positions of the predicted transmembrane spanning domains in AtNCS1 and VvNCS1 overlap the transmembrane spanning domains of FUR4 (Fig. 1A). In addition, key amino acids conserved among NCS1 proteins are also conserved in AtNCS1. Recently, several tertiary structures were resolved for the benyl-hydantoin transporter (Mhp1), a NCS1 from *Microbacterium liquifaciens*, aiding in the development of a molecular dynamic simulation model and the identification of likely solute and cation interacting amino acids [30,31]. AtNCS1 shares 30 of 34 amino acids highly conserved among NCS1 proteins as well as four of six solute interacting amino acids and two of five cation interacting amino acids. Together these data solidly place AtNCS1 in the NCS1 super family.

NCS1 members are ubiquitous in nature and the plant kingdom is no exception. Fig. 1B details a representative phylogenetic tree detailing the relationship between AtNCS1 amino acid sequence and likely orthologous proteins from across the plant and microbial kingdoms. The order of AtNCS1 sequence similarity among orthologous plant proteins mirrors the hierarchy of taxa throughout the plant kingdom showing the highest similarity to dicots (*Vitus, Rincus, Populus* and *Solanum*), followed by monocots (*Zea* and *Oryza*), gymnosperm (*Picea*), nonflowering moss (*Physcomitrella*) and chlorophyte algae (*Chlamydomonas, Osterococcus*). Significant, but more distant similarities are observed between plant NCS1 proteins and orthologous proteins from diverse sources of bacteria (*Escherichia, Plesiocystis, Bacillus, Paracoccus, Synechococcus, Alteromonas,* bacterium *Ellin514*), archaebacteria (*Aeropyrum*), and *S. cerevisiae*. All of the NCS1 proteins locate together in a distinct clade. AtNCS1 is different from other Arabidopsis nucleobase and nucleoside transporters here represented by two members each of the AtNAT, AtUPS, AtENT, AtPUP and AtAZG families (Fig. 1B).

3.2. Molecular characterization of the AtNCS1 locus

The *AtNCS1* locus is among a minority of nuclear genes in the Arabidopsis genome that appears to have no introns. Further this locus contains two in frame ATG codons which predict either a long 1800 bp open reading frame (*orf1*) starting from *ATG-1* that encodes for a 598 amino acid protein, or a shorter 1509 bp ORF (*orf2*) with an origin at *ATG-2* that encodes for a 501 amino acid protein (Fig. 2A). No verified full length cDNA including the long
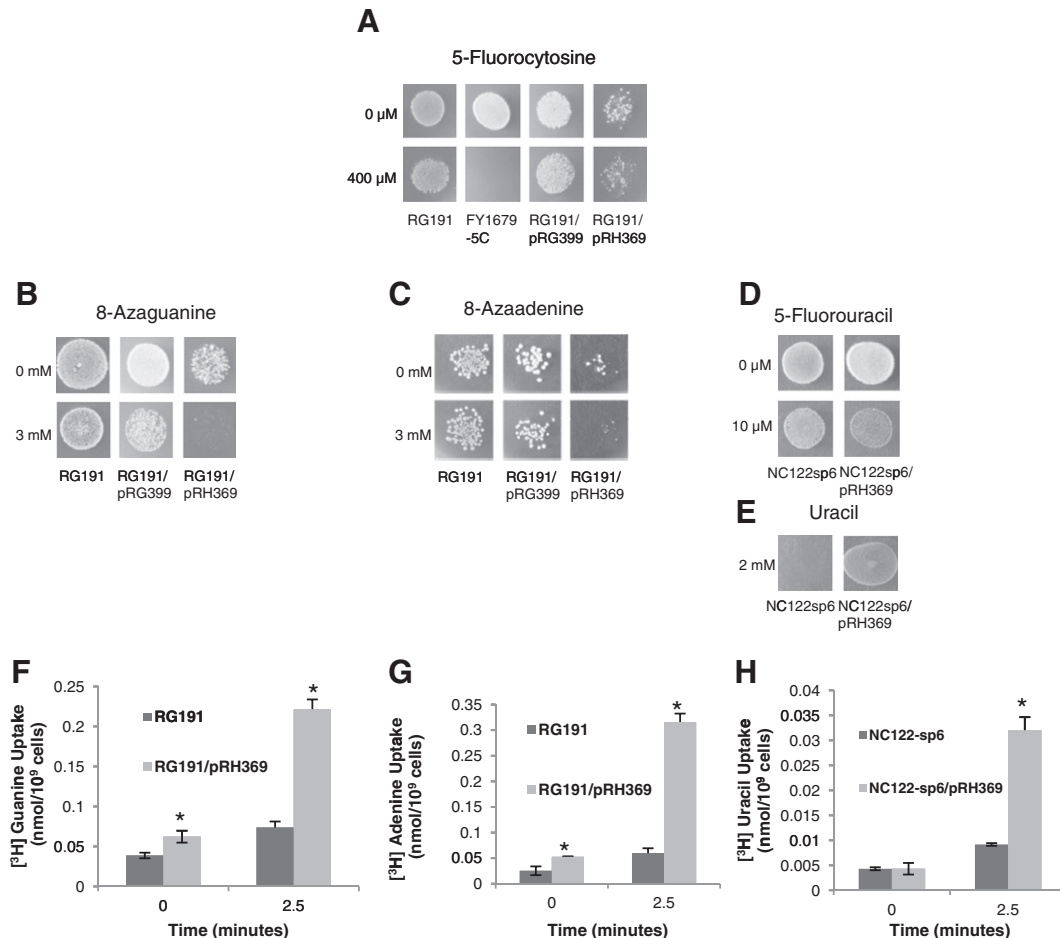

Fig. 5. Growth of *Saccharomyces cerevisiae* expressing *AtNCS1* on toxic purine or pyrimidine analogs and uptake of [³H]-adenine, -guanine, and -uracil. The growth pattern of yeast strains: deficient for the adenine-cytosine transporter *fcy2* (RG191); deficient for the uracil transporter *fur4* (NC122sp6); wild type for *FCY2* and *FUR4* (FY1679-5C); with an empty expression vector (pRG399); or with the *AtNCS1* coding region placed under constitutive transcriptional control (pRH369) were grown on nutrient media with increasing amounts of 5-fluorocytosine (A), 8-azaguanine (B), 8-azaadenine (C) or 5-fluorouracil (D). The growth pattern of NC122sp6 alone or containing pRH369 on nutrient media with uracil as the sole nitrogen source is presented in (E). RG191 and RG 191 + pRH369 were incubated [³H]-adenine, -guanine, or -uracil in citrate buffer (pH 3.5) and aliquots were taken at 0 and 2.5 min. Values shown are the mean of at least three independent experiments. Error bars indicate the standard error of the mean. Statistical analysis used an independent paired *t*-test. Significance was measured at $^*P = 0.05$.

1.8 kb region exists although a few expressed sequence tags containing ATG-1 sequence have been documented in NCBI database. However, full-length clones encompassing the shorter version are available. The possibility two different ORFs ascribed to locus At5g03555 leads to some ambiguity as to the official length. The following indications suggest that the longer protein encoded by orf-1 is the in planta functional version. Several in silico subcellular localization programs predict different locals for the 598 aa AtNCS1: either in the chloroplast (iPSORT; LOCtree; Multiloc and Predotar), mitochondria (MitoPred and TargetP) or plasma membrane (WoLFPSORT) [32–39]. ChloroP predicts a chloroplast transit sequence of 43 amino acids [40]. Given that the chloroplast is a key local for nucleobase biochemistry, plastid membrane localization for AtNCS1 is not unwarranted. Although AtNCS1 sequences are not present in any subcellular Arabidopsis proteomic data bases (including the recent AT-CHLORO database [41], data exists for the AtNCS1 homolog from maize GRMZM2G362848_P01. Here the epitope AIFLLLPSR is found in maize chloroplast outer membrane and thylakoid samples from the Plant Proteome DataBase (http://ppdb.tc.cornell.edu) and is similar to the Arabidopsis protein sequence AIFLLLPGH present only in AtNCS1.

Expression of the gene was verified through RT-PCR analysis using oligonucleotides internal to the ORF (Fig. 2A and D). AtNCS1 is expressed in 5- and 10-day-old seedlings, adult leaf, inflorescence and flowers (Fig. 2D). The RT-PCR expression patterns are consistent with the compiled expression data available through The Arabidopsis Information Resource (e.g. Arabidopsis eFP Browser) [42]. Three independent insertion mutant lines were analyzed. Representative homozygous wild type, heterozygous and homozygous mutant individuals from a segregating family were genotyped by PCR analysis for T-DNA insertion line WiscDsLox419Co3 (Fig. 2A and B). We designated this insertion mutation allele as AtNcs1-1. The DNA insertion in line GK-266G10 locates to +6 bp downstream of ATG-1 and is designated as allele AtNcs1-2 (Fig. 2C). Enhancer trap line ET8162 carries an insertion at +129 bp and is designated as AtNcs1-3 (Fig. 2C). AtNCS1 transcript is detected in leaves homozygous for AtNcs1-2 (data not shown) but is absent from homozygous AtNcs1-1 and AtNcs1-3 leaves (Fig. 2D and E). No difference in visible phenotype and fertility is observed between homozygous AtNcs1-1, AtNcs1-2, AtNcs1-3 and wild type lines of Arabidopsis.

3.3. AtNCS1 null mutants show resistance to certain purine and pyrimidine analogs

Three different homozygous T-DNA insertion mutants in the AtNCS1 locus were tested for their ability to germinate and grow in a range of toxic purine or pyrimidine analog concentrations. In comparison to wild type, homozygous AtNcs1-1 mutants displayed resistance to toxicity of 8-azaadenine, 8-azaguanine, and 5-fluorouracil (Fig. 3A–D). AtNcs1-1 displayed 2.3-fold more resistance to 8-azaguanine than wild type (wild type $I_{50} = 3$ μM; AtNcs1-1 $I_{50} = 7$ μM) (Fig. 3D). However, AtNcs1-1 displayed lower levels of resistance to 8-azaadenine, only 0.7-fold resistance compared to wild type (wild type $I_{50} = 7$ μM; AtNcs1-1 $I_{50} = 10$ μM) (Fig. 3C). This differential level of sensitivity to 8-azaguanine and 8-azaadenine can be clearly demonstrated at 5 μM and 10 μM. For wild type, at 5 μM, seedling fresh weight was 62% of the control in case of 8-azaadenine and only 10% in case of 8-azaguanine while for AtNcs1-1 it was 70% of the control for 8-azaadenine and 43% of the control for 8-azaguanine (Fig. 3C and D). AtNcs1-3 mutant seedlings displayed a growth curve for 8-azaguanine very similar to that of AtNcs1-1 seedlings. AtNcs1-3 was threefold more resistant to 8-azaguanine than wild type (wild type $I_{50} = 4$ μM; AtNcs1-3 $I_{50} = 12$ μM) (Fig. 3F). This result confirms that the 8-azaguanine resistance is not an allele-specific phenomenon but is inherent to the functionality of AtNCS1. As for resistance to 5-fluorouracil,

AtNcs1-1 was twofold more resistant than wild type (wild type $I_{50} = 12$ μM; AtNcs1-1 $I_{50} = 24$ μM) (Fig. 3E). At 20 μM 5-fluorouracil, seedling fresh weight was 55% of the control in AtNcs1-1 and only 30% of the control in wild type (Fig. 3E). In contrast, AtNcs1-1 was as sensitive as the wild type to other nucleoside and nucleobase analogs including 5-fluorocytosine, 5-bromo-2′-deoxyuridine, 5-fluoro-2′-deoxyuridine, 5-fluoroorotic acid and pyrithiamine (a thiamine analogue) (Table 2). The ability to utilize allantoin as a nitrogen source was tested for AtNcs1-1 and wild type seedlings – no difference was observed (Table 2). Seedling growth resistance to some toxic analogs in AtNcs1-1 and AtNcs1-3 is due to the fact that T-DNA insertions in both mutant lines resulted in a knock-out allele with no transcript produced (Fig. 2D and E). Lack of AtNCS1 protein in those two mutant lines may be greatly reducing the amount of toxic analogs taken up by the plant which would explain the observed resistance to some toxic analogs. The AtNcs1-2 mutant line was as sensitive as the wild type to 8-azaguanine (data not shown). This result and the presence of an AtNCS1-specific transcript in mutant tissue resulted in no further investigation of this line.

3.4. In planta radio-labeled nucleobase uptake studies

In planta radiolabeled nucleobase uptake experiments were performed and show that the uptake of [^{3}H]-adenine and -guanine by 11- to 13-day-old seedlings was significantly reduced in AtNcs1-1 compared to Columbia wild type (Fig. 4A). Compared to wild type, AtNcs1-1 uptake of [^{3}H]-guanine was reduced by 50% while uptake of [^{3}H]-adenine was reduced by 40% (Fig. 4A). On the other hand, in seedlings of the same developmental stage uptake of [^{3}H]-uracil was significantly reduced in the wild type compared to AtNcs1-1 (Fig. 4B). Uptake of [^{3}H]-uracil by wild type was reduced by about 20% when compared to AtNcs1-1 (Fig. 4B). This seemingly contradictory result suggests that AtNCS1 may not act as the main transport route for uracil at this developmental stage, but that other transporters are then more active. Indeed AtUPS1 and 2 and to a lesser extent AtAzgA2 transport uracil [12,19]. Expression data shows that 11- to 13-day-old seedlings have appreciable AtUPS2 expression whereas 5- to 7-day-old seedlings have signifi-
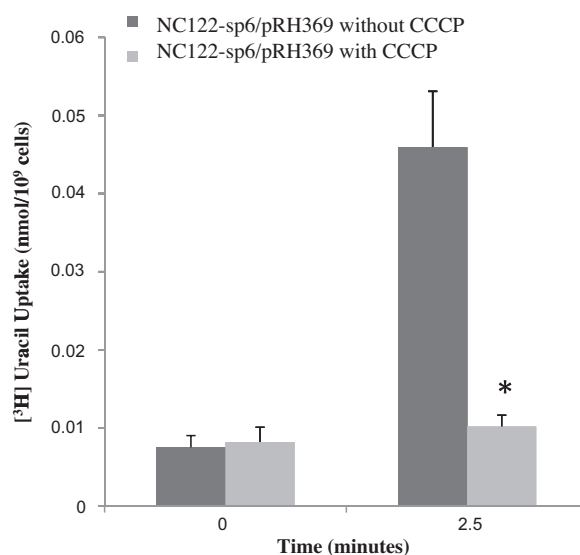

Fig. 6. [^{3}H]-uracil uptake by *Saccharomyces cerevisiae* expressing *AtNCS1*. Yeast strain NC122-sp6 deficient in the uptake of uracil and containing pRH369 was incubated with [5,6-^{3}H]uracil in the presence or absence of protonophore CCCP and aliquots were taken at 0 and 2.5 min. Values shown are the mean of at least three independent experiments. Error bars indicate the standard error of the mean. Statistical analysis used an independent paired t-test. Significance was measured at $^*P = 0.05$.

cantly less expression of AtUPS1 and 2 when *AtNCS1* is expressed (Fig. 2D) [12]. Radiolabel uracil uptake experiments were conducted with 5-day-old seedlings and revealed that *AtNcs1-1* accumulates a significantly smaller amount of [³H]-uracil compared to wild type (Fig. 4C). The result suggests that AtNCS1 is an important source of uracil transport in 5- to 7-day-old seedlings. Interestingly at germination and the first week of seedling development, nucleobase salvage – particularly uracil salvage – is essential for seedling development with strong expression of genes encoding pyrimidine salvage enzymes [6,7,43]. As the seedling develops after this initial stage there is a shift toward de novo pyrimidine synthesis and recycling of pyrimidine nucleotides increases [43,44]. The shift in the rate of nucleobase salvage/synthesis versus catabolism may also be reflected in the presence and activities of different nucleobase transporters. It appears that at 11 days, uracil transport in the seedling relies less on AtNCS1 and more on AtUPS2 or other transporters.

3.5. Heterologous complementation studies confirm that AtNCS1 is a nucleobase transporter

Heterologous complementation studies in *S. cerevisiae* were performed to test whether AtNCS1 could act in a transport capacity outside of a plant. Yeast expression plasmids containing Arabidopsis At5g03555 sequences which encode for a long AtNCS1 protein of 598 amino acids, pRH124, and sequences encoding for a short AtNCS1 protein of 501 amino acids, pRH369, were transformed into two yeast strains deficient in either *fcy2* (adenine–cytosine–guanine transport) or *fur4* (uracil transport). The short version encodes for a 502 amino acid protein devoid of predicted chloroplast transit and signal sequences present in the first ∼99 amino acids. Yeast strains deficient for *fcy2* and harboring either pRH124 (data not shown) or pRH369 (Fig. 5B and C) displayed heightened sensitivity to growth on 8-azaadenine, 8-azaguanine. However, strains harboring pRH369 displayed appreciably more sensitivity than those harboring pRH124, suggesting that either the shorter AtNCS1 protein functions better in yeast and/or that there is a steady state higher level of AtNCS1 short protein compared to long AtNCS1 in the respective strains. Although it is evident that both the long and short AtNCS1 forms function in yeast, further characterization was conducted with yeast strains harboring pRH369.

The yeast expression vector pRH369 containing sequences encoding for a short AtNCS1 protein was transformed into two yeast strains deficient in either *fcy2* (adenine-cytosine-guanine transport) or *fur4* (uracil transport). Yeast strains were grown on media containing 5-fluorocytosine, 8-azaadenine, 8-azaguanine, 5-fluorouracil or with uracil as the sole nitrogen source. Results shown in Fig. 5 indicate that yeast stains harboring pRH369 regain
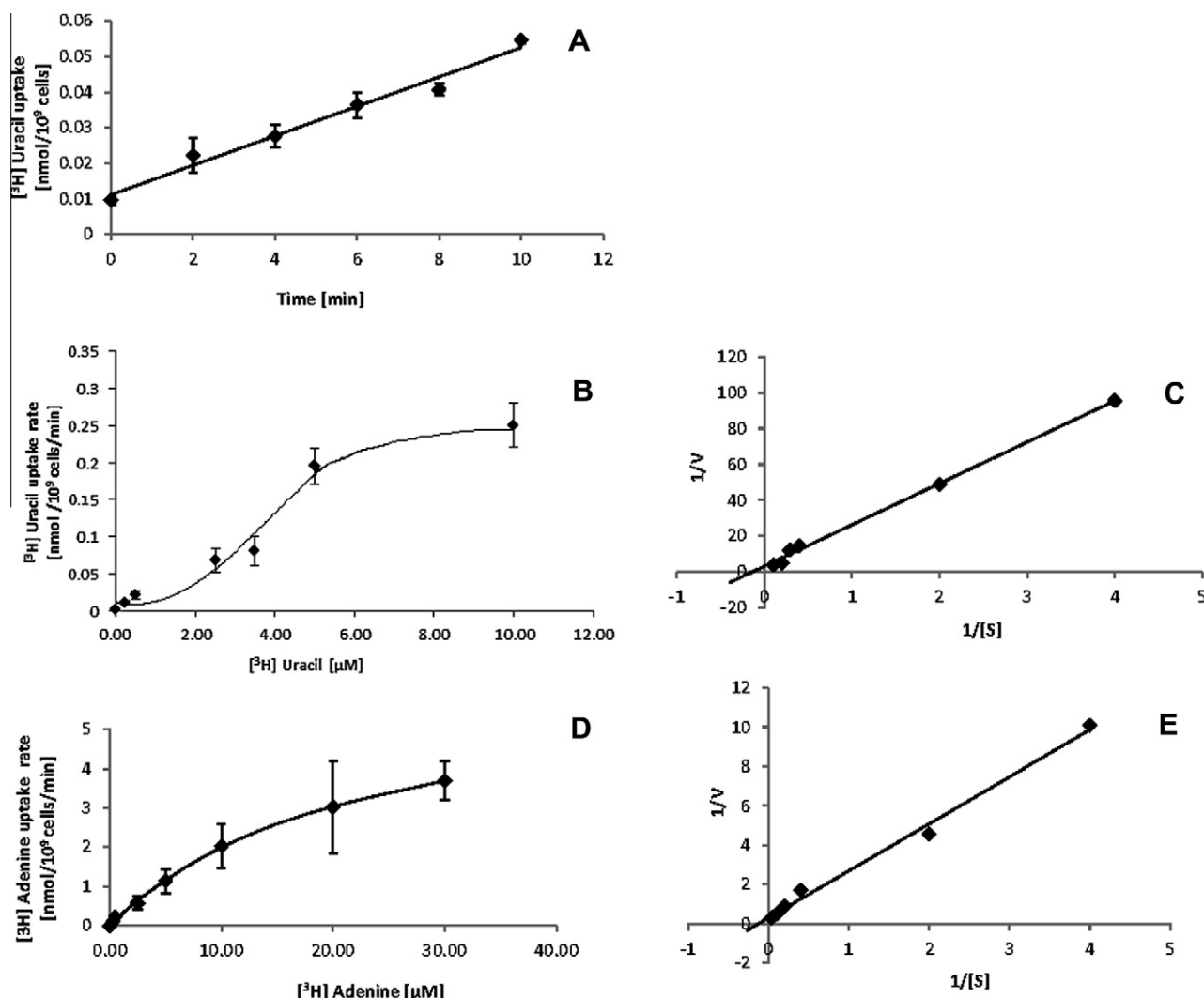

Fig. 7. Substrate kinetics of AtNCS1 expressed in yeast. (A) Time course of the transport of [5,6-³H]uracil. (B) Transport rate of varying concentrations of [5,6-³H]uracil. (C) Lineweaver–Burk plot for [5,6-³H]uracil uptake shown in (B). (D) Transport rate of varying concentrations of [2,8-³H]adenine. (E) Lineweaver–Burk plot for [2,8-³H]adenine uptake shown in (D).

sensitivity to growth on 8-azaguanine, 8-azaadenine and 5-fluoro-uracil, but not to growth on 5-fluorocytosine when compared to control strains deficient in *fcy2* or *fur4* (Fig. 5A–D). The uracil transport-deficient yeast stain is unable to grow on uracil as a sole nitrogen source but regains this ability with pRH369 (Fig. 5E). Additionally, yeast strains deficient in *fur4* or *fcy2* and transformed with pRH369 showed significantly increased uptake of [^{3}H]-guanine, [^{3}H]-adenine as well as [^{3}H]-uracil when compared to the control (Fig. 5F–H). These results match the toxic analog growth studies and radio-labeled nucleobase uptakes studies in planta.

In the presence of the protonophore CCCP, [^{3}H]-uracil uptake by the yeast strain deficient in *fur 4* and harboring pRH369 is strongly inhibited (Fig. 6). This result is consistent with AtNCS1 functioning as a nucleobase cation symporter.

A time course experiment for [^{3}H]-uracil uptake by yeast expressing pRH369 revealed a linear relationship up to 10 min (Fig. 7A). As we have shown here AtNCS1 displays a distinct solute transport from fungal NCS1 proteins. AtNCS1 transports guanine, adenine, and uracil (Figs. 4 and 5) whereas fungal NCS1 proteins transport either guanine and adenine (FCY2) or uracil (FUR4). Because of that we examined the transport kinetics of [^{3}H]-adenine and [^{3}H]-uracil in yeast cells expressing pRH369 at 2.5 min when the uptake of [^{3}H]-uracil was within the linear range (Fig. 7A). Increasing [^{3}H]-uracil and [^{3}H]-adenine concentrations showed an initial linear rate but approached saturation at higher concentrations (Fig. 7B and D). Lineweaver–Burk plots revealed Km_{app} = 7.0 μM and V_{max} = 0.3 (nmol/10^9 cells/min) for uracil (Fig. 7C) and Km_{app} = 7.9 μM and V_{max} = 3.3 (nmol/10^9 cells/min) for adenine (Fig. 7E).

Acknowledgements

References

[1] Ross, C.W. (1991) Biosynthesis of nucleotides in: The Biochemistry of Plants (Stumpf, P.K. and Conn, E.E., Eds.), pp. 169–205, Academic Press, New York, NY.

[2] Moffatt, B.A. and Ashihara, H. (2002) Purine and pyrimidine nucleotide synthesis and metabolism in: The Arabidopsis Book (Somerville, C.R. and Meyerowitz, E.M., Eds.), pp. 1–20, Book American Society of Plant Biologists, Rockville, MD. doi/10.1199/tab.0018, http://www.aspb.org/publications/arabidopsis.

[3] Kafer, C., Zhou, L., Santoso, D., Guirgis, A., Weers, B., Park, S. and Thornburg, R. (2004) Regulation of pyrimidine metabolism in plants. Front. Biosci. 9, 1611–1625.

[4] Zrenner, R., Stitt, M., Sonnewald, U. and Boldt, R. (2006) Pyrimidine and purine biosynthesis and degradation in plants. Annu. Rev. Plant Biol. 57, 805–836.

[5] Kombrink, E. and Beevers, H. (1983) Transport of purine and pyrimidine bases and nucleosides from endosperm to cotyledons in germinating castor bean seedlings. Plant Physiol. 73, 370–376.

[6] Stasolla, C., Katahira, R., Thorpe, T.A. and Ashihara, H. (2003) Purine and pyrimidine nucleotide metabolism in higher plants. J. Plant Physiol. 160, 1271–1295.

[7] Mainguet, S.E., Gakière, B., Majira, A., Pelletier, S., Bringel, F., Guérard, F., Caboche, M., Berthomé, R. and Renou, J.P. (2009) Uracil salvage is necessary for early Arabidopsis development. Plant J. 60, 280–291.

[8] Gillissen, B., Bürkle, L., André, B., Kühn, C., Rentsch, K., Brandl, B. and Frommer, W.B. (2000) A new family of high-affinity transporters for adenine, cytosine, and purine derivatives in Arabidopsis. Plant Cell 12, 291–300.

[9] Bürkle, L., Cedzich, A., Dopke, C., Stransky, H., Okumoto, S., Gillissen, B., Kuhn, C. and Frommer, W.B. (2003) Transport of cytokinins mediated by purine transporters of the PUP family expressed in phloem, hydathodes, and pollen of Arabidopsis. Plant J. 34, 13–26.

[10] Cedzich, A., Stransky, H., Schulz, B. and Frommer, W.B. (2008) Characterization of cytokinin and adenine transport in Arabidopsis cell cultures. Plant Physiol. 148, 1857–1867.

[11] Desimone, M., Catoni, E., Ludewig, U., Hilpert, M., Schneider, A., Kunze, R., Tegeder, M., Frommer, W.B. and Schumacher, K. (2002) A novel superfamily of transporters for allantoin and other oxo-derivatives of nitrogen heterocyclic compounds in Arabidopsis. Plant Cell 14, 847–856.

[12] Schmidt, A., Su, Y.H., Kunze, R., Warner, S., Hewitt, M., Slocum, R.D., Ludewig, U., Frommer, W.B. and Desimone, M. (2004) UPS1 and UPS2 from Arabidopsis mediate high affinity transport of uracil and 5-fluorouracil. J. Biol. Chem. 279, 44817–44824.

[13] Schmidt, A., Baumann, N., Schwarzkopf, A., Frommer, W.B. and Desimone, M. (2006) Comparative studies on ureide permeases in Arabidopsis thaliana and analysis of two alternative splice variants of AtUPS5. Planta 224, 1329–1340.

[14] Pélissier, H.C., Frerich, A., Desimone, M., Schumacher, K. and Tegeder, M. (2004) PvUPS1, an allantoin transporter in nodulated roots of French bean. Plant Physiol. 134, 664–675.

[15] De Koning, H. and Diallinas, G. (2000) Nucleobase transporters. Mol. Membr. Biol. 17, 75–94.

[16] Pantazopoulou, A. and Diallinas, G. (2007) Fungal nucleobase transporters. FEMS Microbiol. Rev. 31, 657–675.

[17] Schultes, N.P., Brutnell, T.P., Allen, A., Dellaporta, S.L., Nelson, T. and Chen, J. (1996) The *leaf permease 1* gene of maize is required for chloroplast development. Plant Cell 8, 463–475.

[18] Argyrou, E., Sophianopoulou, V., Schultes, N. and Diallinas, G. (2001) Functional characterization of a maize purine transporter by expression in Aspergillus nidulans. Plant Cell 13, 953–964.

[19] Mansfield, T.A., Schultes, N.P. and Mourad, G.S. (2009) AtAzg1 and AtAzg2 comprise a novel family of purine transporters in Arabidopsis. FEBS Lett. 583, 481–486.

[20] Jund, R., Weber, E. and Chevallier, M.R. (1988) Primary structure of the uracil transport protein of Saccharomyces cerevisiae. Eur. J. Biochem. 171, 417–424.

[21] Woody, S.T., Austin-Phillips, S., Amasino, R.M. and Krysan, P.J. (2007) The WiscDsLox T-DNA collection: an Arabidopsis community resource generated by using an improved high-throughput T-DNA sequencing pipeline. J. Plant Res. 120, 157–165.

[22] Rosso, M.G., Li, Y., Strizhov, N., Reiss, B., Dekker, K. and Weisshaar, B. (2003) An Arabidopsis thaliana T-DNA mutagenized population (GABI-Kat) for flanking sequence tag-based reverse genetics. Plant Mol. Biol. 53, 247–259.

[23] Sundaresan, V., Springer, P., Volpe, T., Haward, S., Jones, J.D.G., Dean, C., Ma, H. and Martienssen, R.A. (1995) Patterns of gene action in plant development revealed by enhancer trap and gene trap transposable elements. Genes Dev. 9, 1797–1810.

[24] Wagner, R., de Montigny, J., de Wergifosse, P., Souciet, J.L. and Potier, S. (1998) The ORF YBL042 of Saccharomyces cerevisiae encodes a uridine permease. FEMS Microbiol. Lett. 159, 69–75.

[25] Winzeler, E.A., Shoemaker, D.D., Astromoff, A., Liang, H., Anderson, K., André, B., Bangham, R., Benito, R., Boeke, J.D., Bussey, H., Chu, A.M., Connelly, C., Davis, K., Dietrich, F., Dow, S.W., Bakkoury, M.E., Foury, F., Friend, S.H., Gentalen, E., Giaever, G., Hegemann, J.H., Jones, T., Laub, M., Liao, H. and Davis, R.W. (1999) Functional characterization of the S. cerevisiae genome by gene deletion and parallel analysis. Science 285, 901–906.

[26] Gietz, R.D. and Woods, R.A. (2002) Transformation of yeast by the LiAc/ss carrier DNA method. Methods Enzymol. 350, 87–96.

[27] André, B. (1995) An overview of membrane transport proteins in Saccharomyces cerevisiae. Yeast 11, 1575–1611.

[28] Stolz, J. and Vielreicher, M. (2003) Tpn1p, the plasma membrane vitamin B6 transporter of Saccharomyces cerevisiae. J. Biol. Chem. 278, 18990–18996.

[29] Krogh, A., Larsson, B., von Heijne, G. and Sonnhammer, E.L.L. (2001) Predicting transmembrane protein topology with a hidden markov model: application to complete genomes. J. Mol. Biol. 305, 567–580.

[30] Weyand, S., Shimamura, T., Yajima, S., Suzuki, S., Mirza, O., Krusong, K., Carpenter, E.P., Rutherford, N.G., Hadden, J.M., O'Reilly, J., Ma, P., Saidijam, M., Patching, S.G., Hope, R.J., Norbertczak, H.T., Roach, P.C.J., Iwata, S., Henderson, P.J.F. and Cameron, A.D. (2008) Structure and molecular mechanism of a nucleobase-cation-symport-1 family transporter. Science 322, 709–713.

[31] Shimamura, T., Weyand, S., Beckstein, O., Rutherford, N.G., Hadden, J.M., Sharples, D., Sansom, M.S.P., Iwata, S., Henderson, P.J.F. and Cameron, A.D. (2010) Molecular basis of alternating access membrane transport by the sodium-hydantoin transporter Mhp1. Science 328, 470–473.

[32] Emanuelsson, O., Nielsen, H., Brunak, S. and von Heijne, G. (2000) Predicting subcellular localization of proteins based on their N-terminal amino acid sequence. J. Mol. Biol. 300, 1005–1116.

[33] Hua, S. and Sun, Z. (2001) Support vector machine approach for protein subcellular localization prediction. Bioinformatics 17, 721–728.

[34] Bannai, H., Tamada, Y., Maruyama, O., Nakai, K. and Miyano, S. (2002) Extensive feature detection of N-terminal protein sorting signals. Bioinformatics 18, 298–305.

[35] Guda, C., Guda, P., Fahy, E. and Subramanian, S. (2004) MITOPRED: a web server for the prediction of mitochondrial proteins. Nucleic Acids Res. (July 1), 32 (Web Server issue):W372-4. PubMed.

[36] Small, I., Peeters, N., Legeai, F. and Lurin, C. (2004) Predotar: a tool for rapidly screening proteomes for N-terminal targeting sequences. Proteomics 4, 1581–1590.

[37] Nair, R. and Rost, B. (2005) Mimicking cellular sorting improves prediction of subcellular localization. J. Mol. Biol. 348, 85–100.

[38] Höglund, A., Dönnes, P., Blum, T., Adolph, H.W. and Kohlbacher, O. (2006) MultiLoc: prediction of protein subcellular localization using N-terminal targeting sequences, sequence motifs and amino acid composition. Bioinformatics 22, 1158–1165.

[39] Horton, P., Park, K., Obayashi, T., Fujita, N., Harada, H., Adams-Collier, C.J. and Nakai, K. (2007) WoLF PSORT: protein localization predictor. Nucleic Acids Res. 35 (Suppl. 2), W585–W587.

[40] Emanuelsson, O., Nielsen, H. and von Heijne, G. (1999) ChloroP, a neural network-based method for predicting chloroplast transit peptides and their cleavage sites. Protein Sci. 8, 978–984.

[41] Ferro, M., Brugière, S., Salvi, D., Seigneurin-Berny, D., Court, M., Moyet, L., Ramus, C., Miras, S., Mellal, M., Le Gall, S., Kieffer-Jaquinod, S., Bruley, C., Garin, J., Joyard, J., Masselon, C. and Rolland, N. (2010) AT_CHLORO, a comprehensive chloroplast proteome database with subplastidial localization and curated information on envelope proteins. Mol. Cell. Proteomics 9, 1063–1084.

[42] Winter, D., Vinegar, B., Nahal, H., Ammar, R., Wilson, G.V. and Provart, N.J. (2007) An "electronic fluorescent pictograph" browser for exploring and analyzing large-scale biological data sets. PLoS ONE 2 (8), e718, http://dx.doi.org/10.1371/journal.pone.0000718.

[43] Zrenner, R., Riegler, H., Marquard, C.R., Lange, P.R., Geserick, C., Bartosz, C.E., Chen, C.T. and Slocum, R.D. (2009) A functional analysis of the pyrimidine catabolic pathway in Arabidopsis. New Phytol. 183, 117–132.

[44] Jung, H.W., Tschaplinski, T.J., Wang, L., Glazebrook, J. and Greenberg, J.T. (2009) Priming in systemic plant immunity. Science 324, 89–91.

[45] Thompson, J.D., Higgins, D.G. and Gibson, T.J. (1994) CLUSTAL W: improving the sensitivity of progressive multiple sequence alignment through sequence weighting, position-specific gap penalties and weight matrix choice. Nucleic Acids Res. 22, 4673–4680.

[46] Dereeper, A., Guignon, V., Blanc, G., Audic, S., Buffet, S., Chevenet, F., Dufayard, J.F., Guindon, S., Lefort, V., Lescot, M., Claverie, J.M. and Gascuel, O. (2008) Phylogeny.fr: robust phylogenetic analysis for the non-specialist. Nucleic Acids Res. 1, 36.

[47] Edgar, R.C. (2004) MUSCLE: multiple sequence alignment with high accuracy and high throughput. Nucleic Acids Res. 325, 1792–1797.

[48] Guindon, S. and Gascuel, O. (2003) A simple, fast, and accurate algorithm to estimate large phylogenies by maximum likelihood. Syst. Biol. 525, 696–704.

[49] Anisimova, M. and Gascuel, O. (2006) Approximate likelihood ratio test for branches: a fast, accurate and powerful alternative. Syst. Biol. 55, 539–552.

[50] Chevenet, F., Brun, C., Banuls, A.L., Jacq, B. and Chisten, R. (2006) TreeDyn: towards dynamic graphics and annotations for analyses of trees. BMC Bioinformatics 10, 439.